Figure S1. Tree topology based on maximum likelihood analysis of 136 orthologs (Matrix 1). Numbers on nodes indicate bootstrap resampling frequencies.

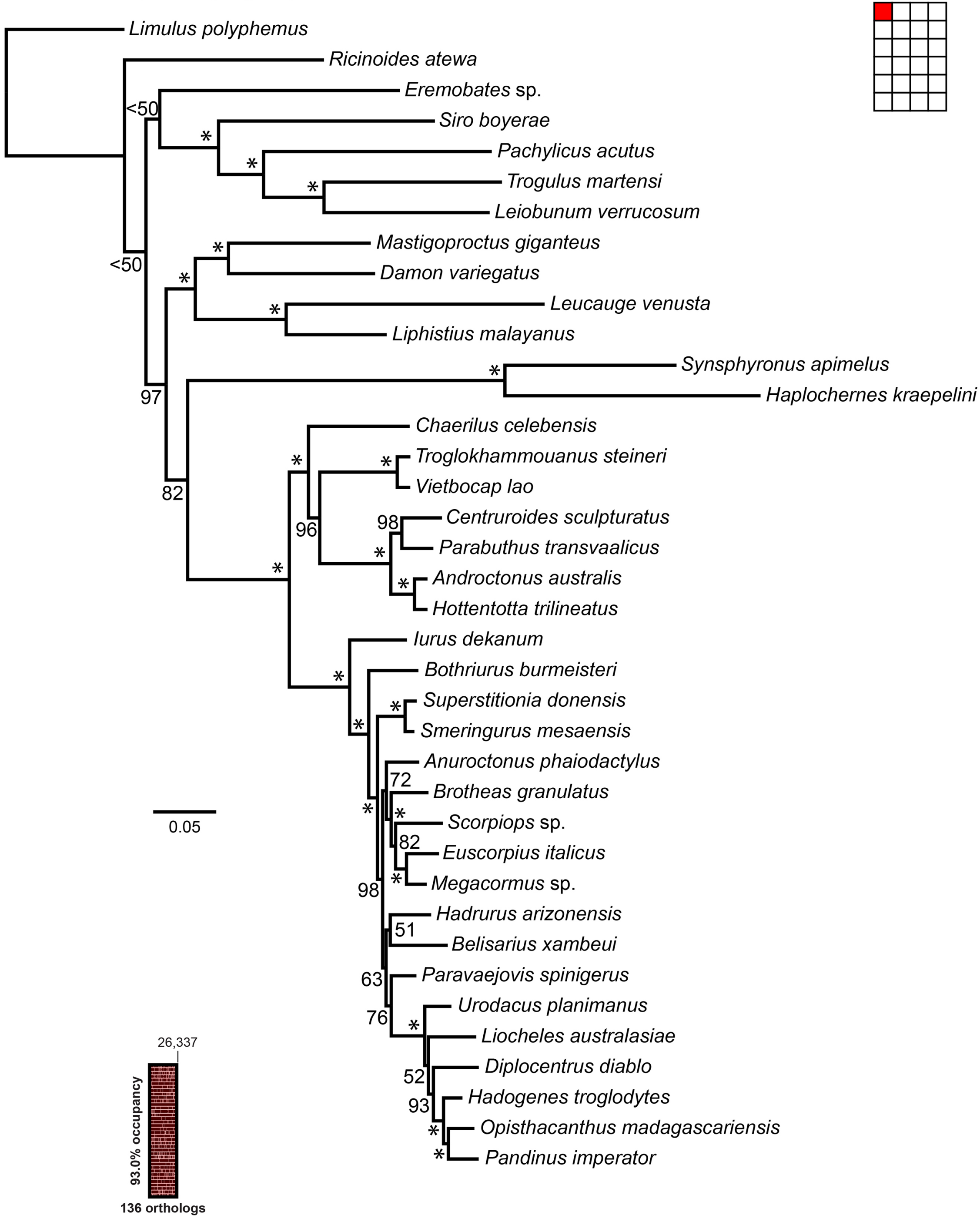

Figure S2. Tree topology based on maximum likelihood analysis of 599 orthologs (Matrix 2). Numbers on nodes indicate bootstrap resampling frequencies.

Figure S3. Tree topology based on maximum likelihood analysis of 1,557 orthologs (Matrix 3). Numbers on nodes indicate bootstrap resampling frequencies.

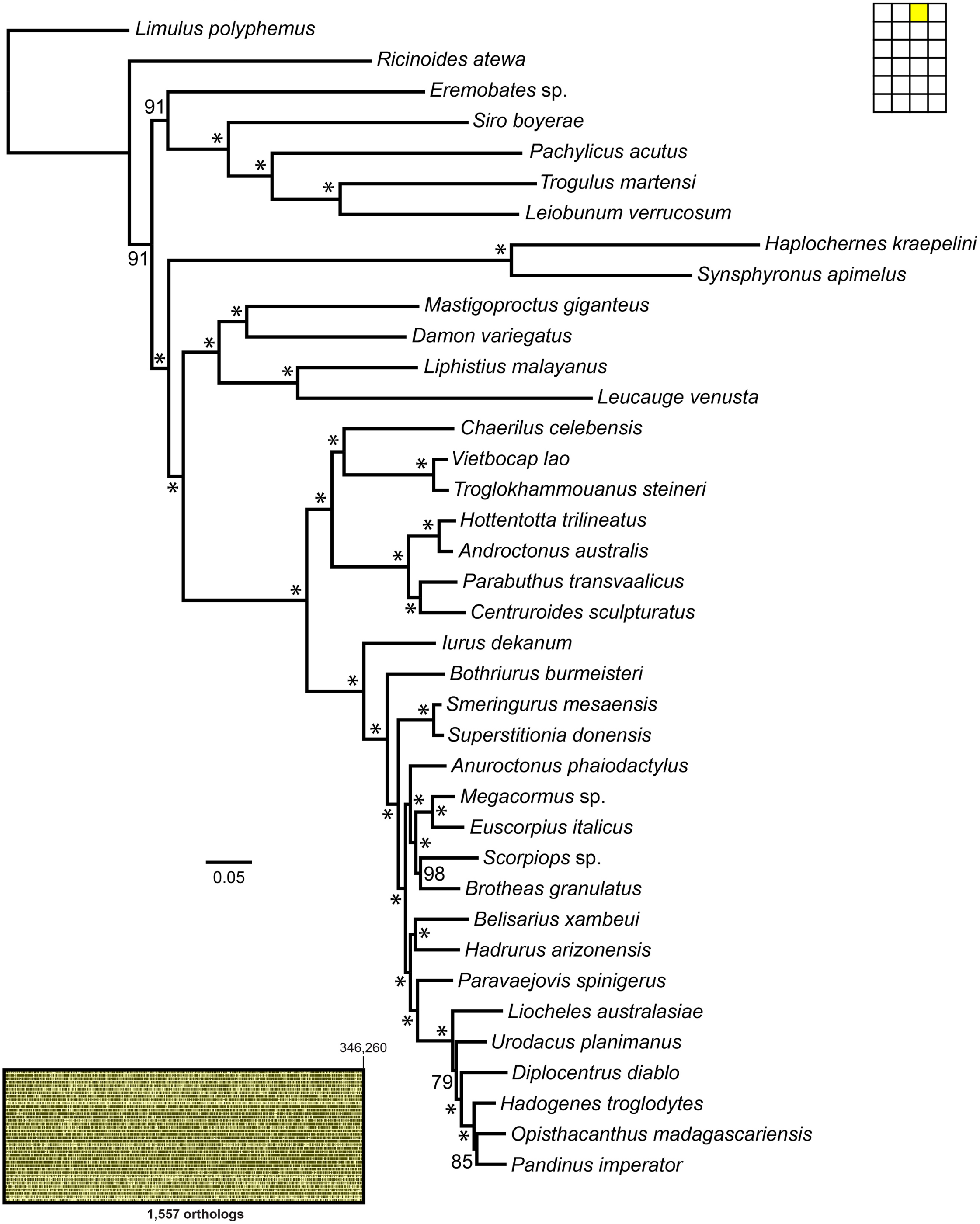

Figure S4. Tree topology based on maximum likelihood analysis of 5,025 orthologs (Matrix 4). Numbers on nodes indicate bootstrap resampling frequencies.

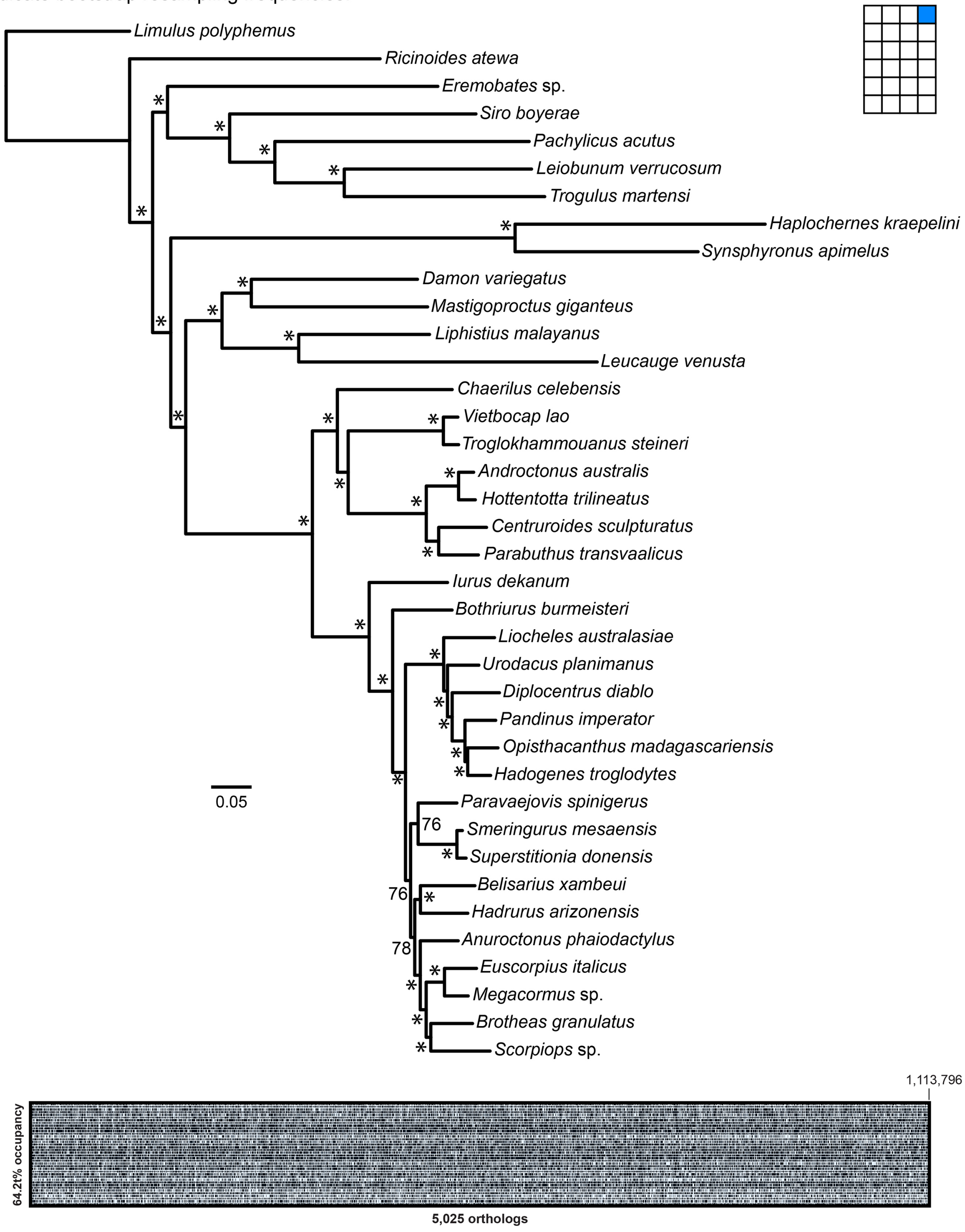

Figure S5. Tree topologies based on species tree methods, analysis of gene trees from Matrix 1. (a) STAR method; (b) NJst method; (c) MP-est method.

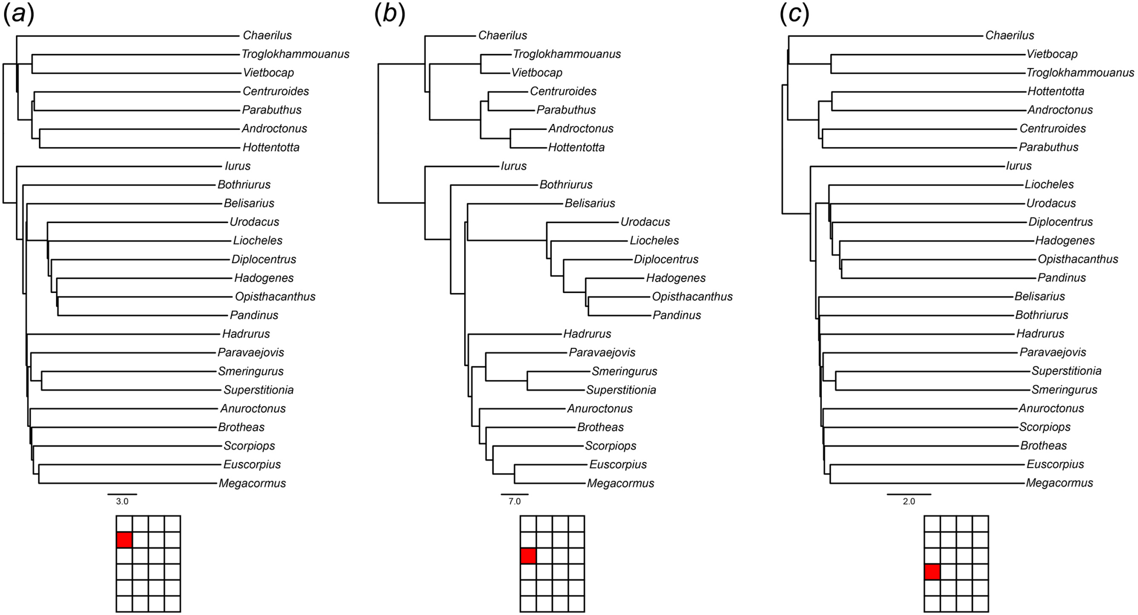

Figure S6. Tree topologies based on species tree methods, analysis of gene trees from Matrix 2. (a) STAR method; (b) NJst method; (c) MP-est method.

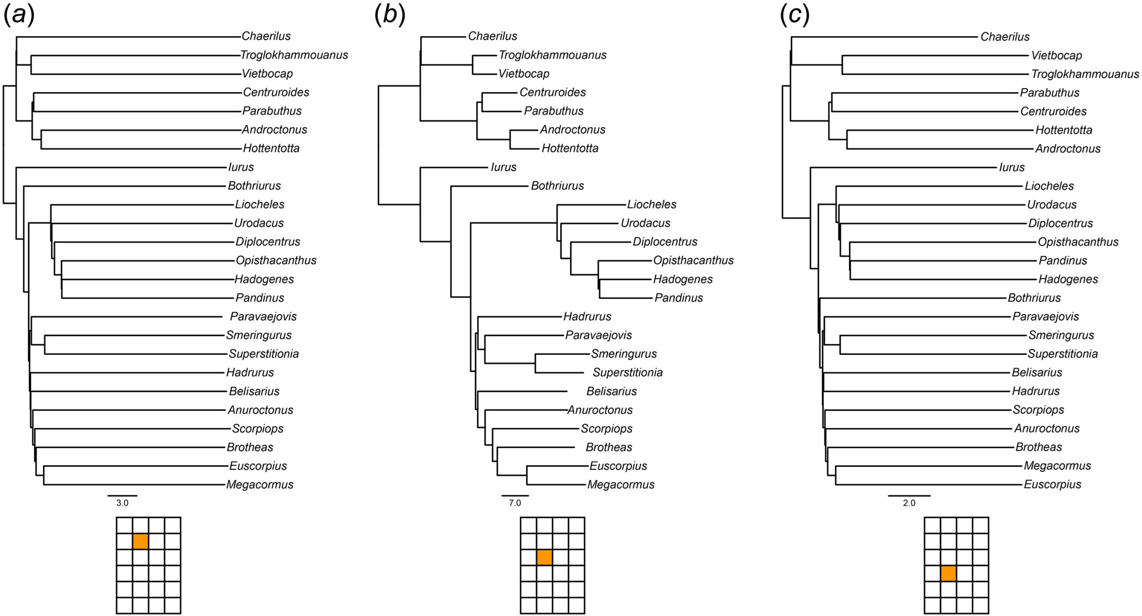

Figure S7. Tree topology based on maximum likelihood analysis of 131 orthologs (Matrix 5). Numbers on nodes indicate bootstrap resampling frequencies.

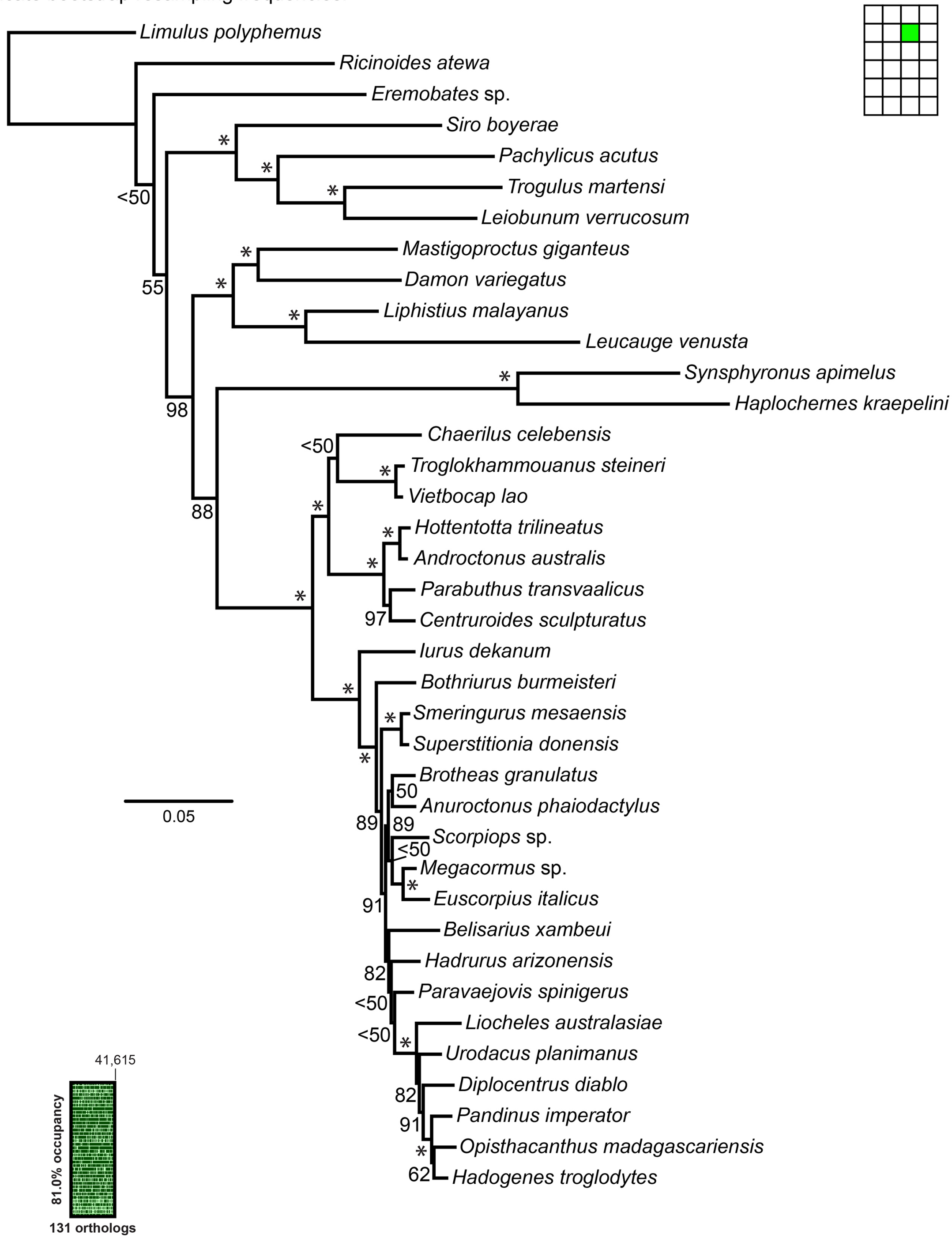

Figure S8. Tree topology based on maximum likelihood analysis of 453 orthologs (Matrix 6). Numbers on nodes indicate bootstrap resampling frequencies.

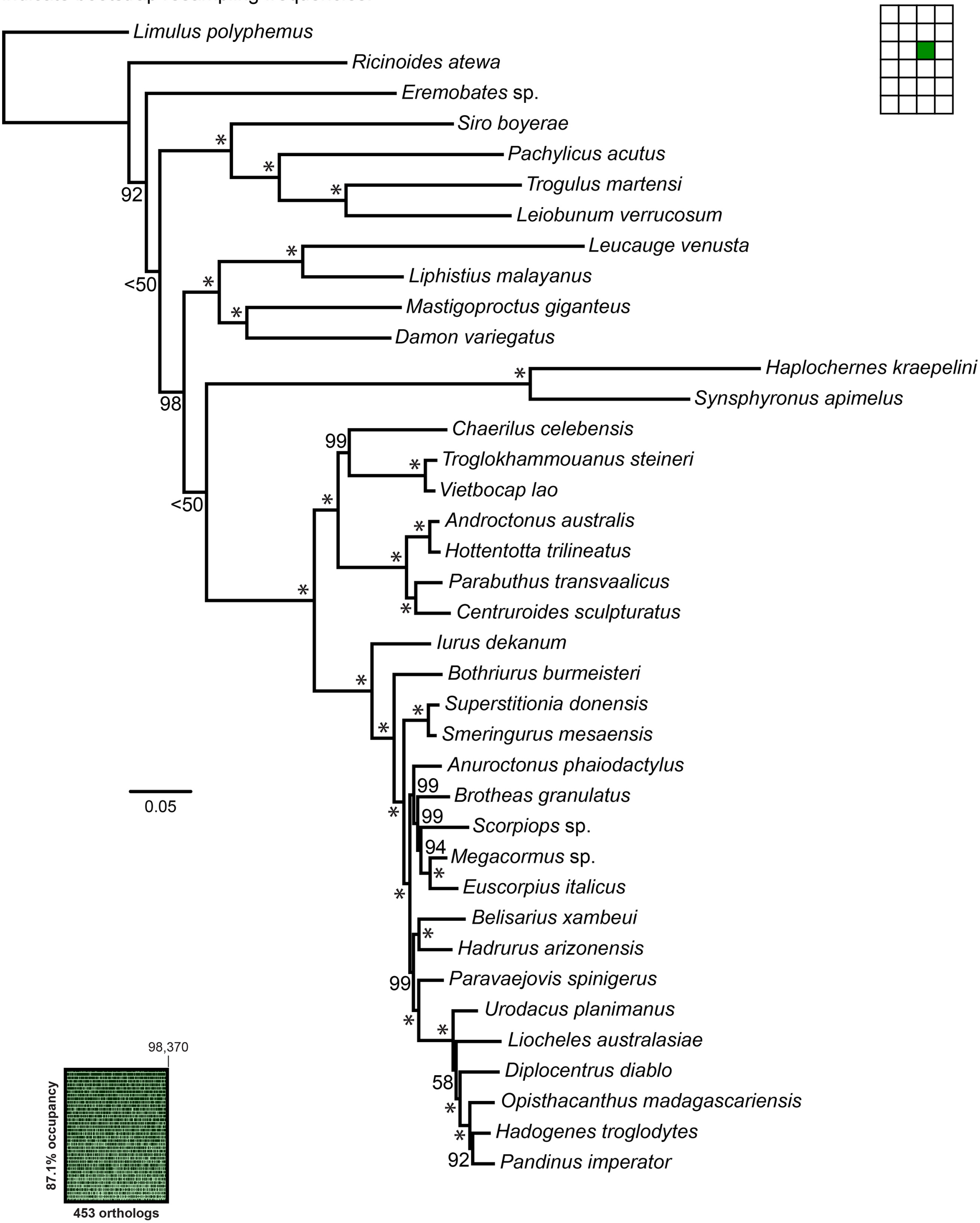

Figure S9. Tree topology based on maximum likelihood analysis of 2,580 orthologs (Matrix 7). Numbers on nodes indicate bootstrap resampling frequencies.

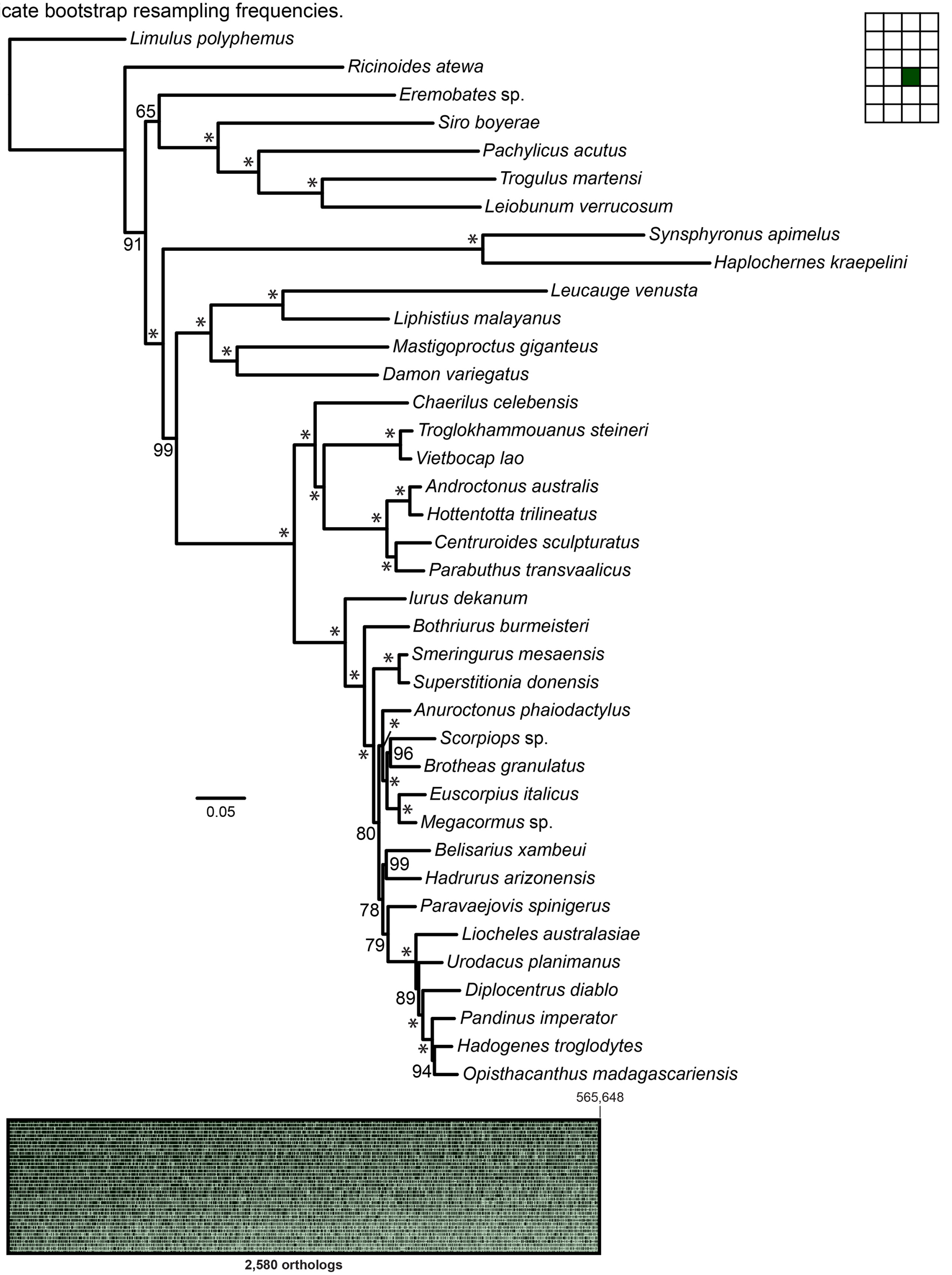

Figure S10. Tree topology based on maximum likelihood analysis of 500 orthologs (Matrix 8). Numbers on nodes indicate bootstrap resampling frequencies.

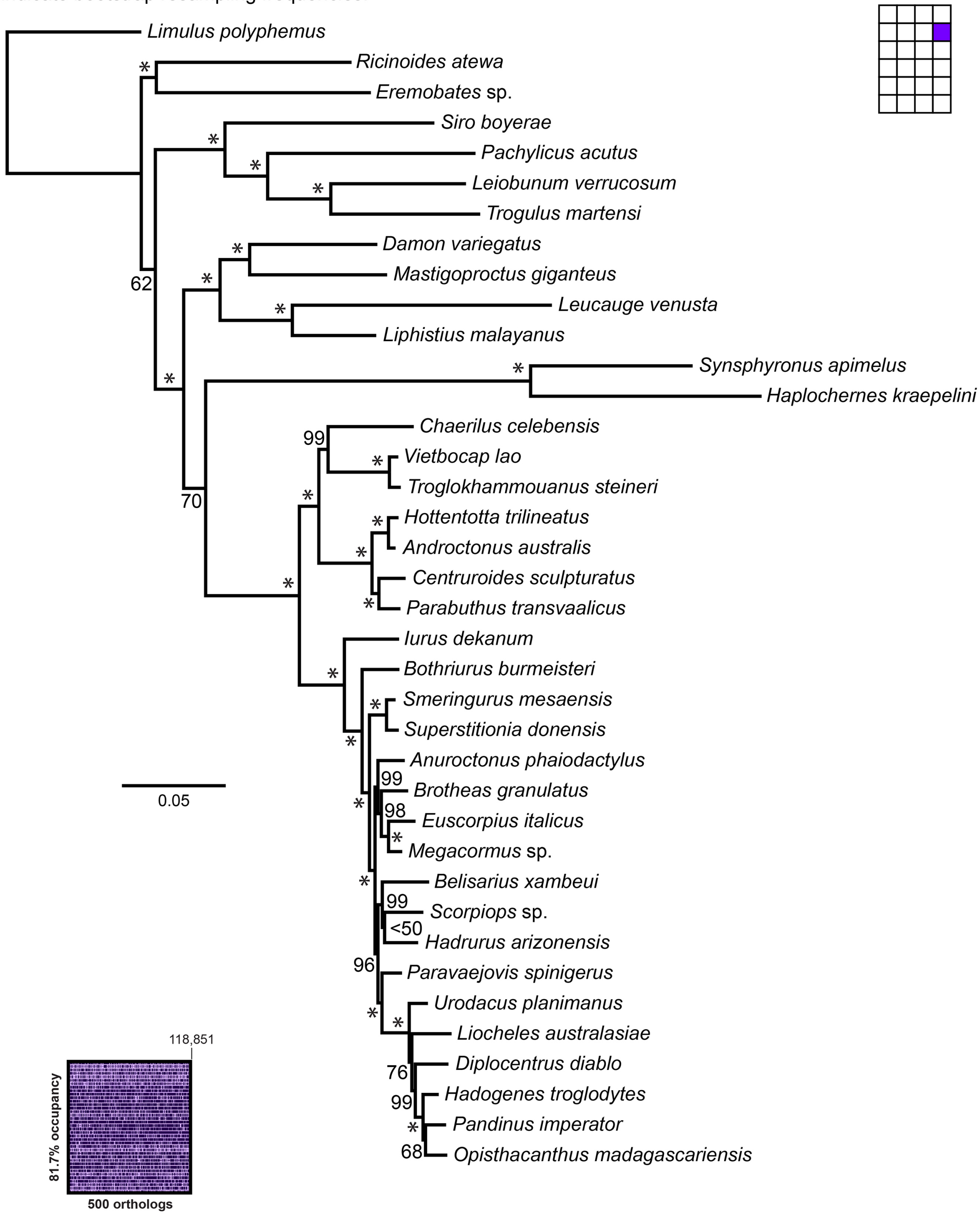

Figure S11. Tree topology based on maximum likelihood analysis of 500 orthologs (Matrix 9). Numbers on nodes indicate bootstrap resampling frequencies.

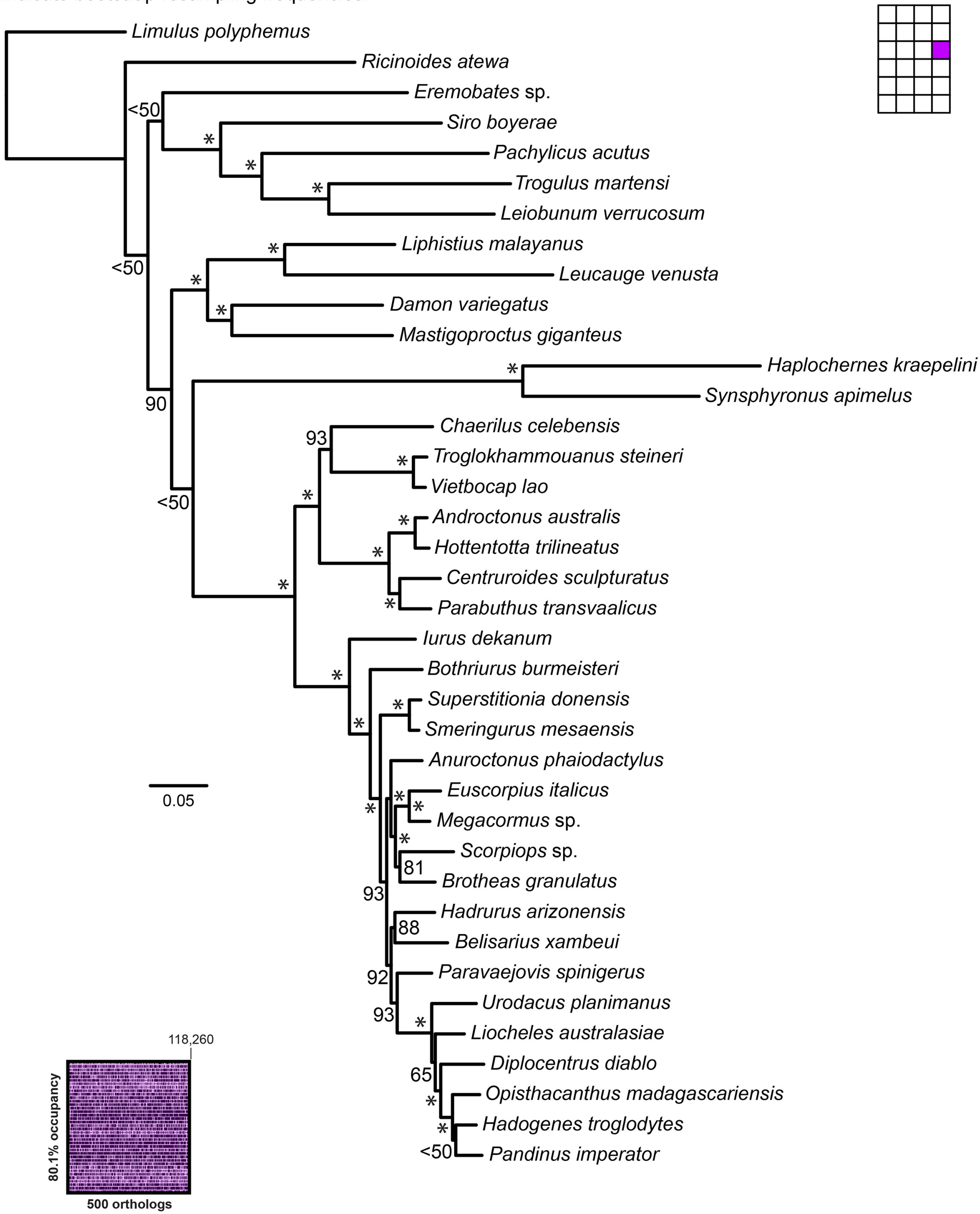

Figure S12. Tree topology based on maximum likelihood analysis of 577 orthologs (Matrix 10). Numbers on nodes indicate bootstrap resampling frequencies.

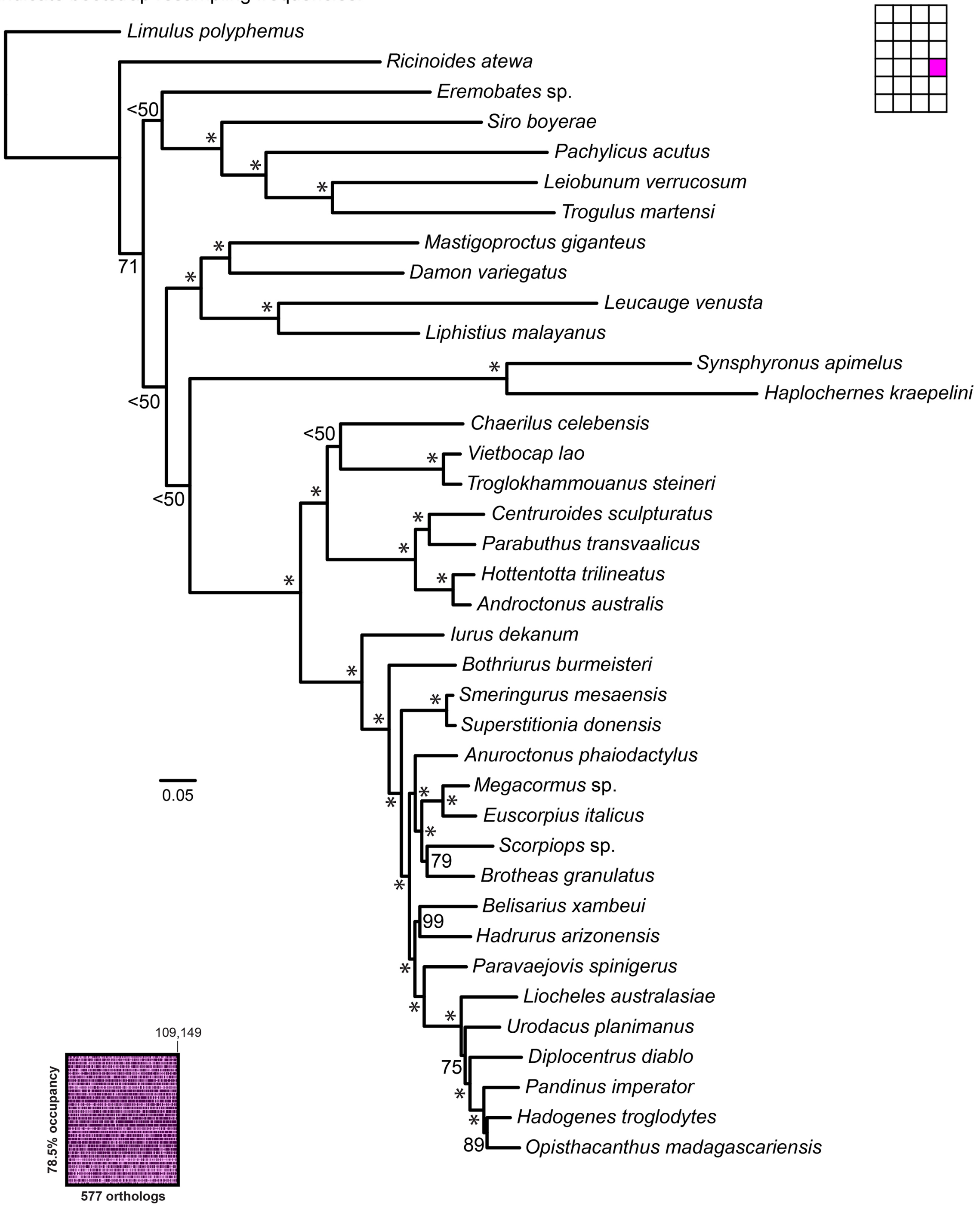

Figure S13. Tree topology based on Bayesian inference analysis of 136 orthologs (Matrix 1). Numbers on nodes indicate posterior probabilities. Unlabelled nodes correspond to posterior probabilities of 1.00.

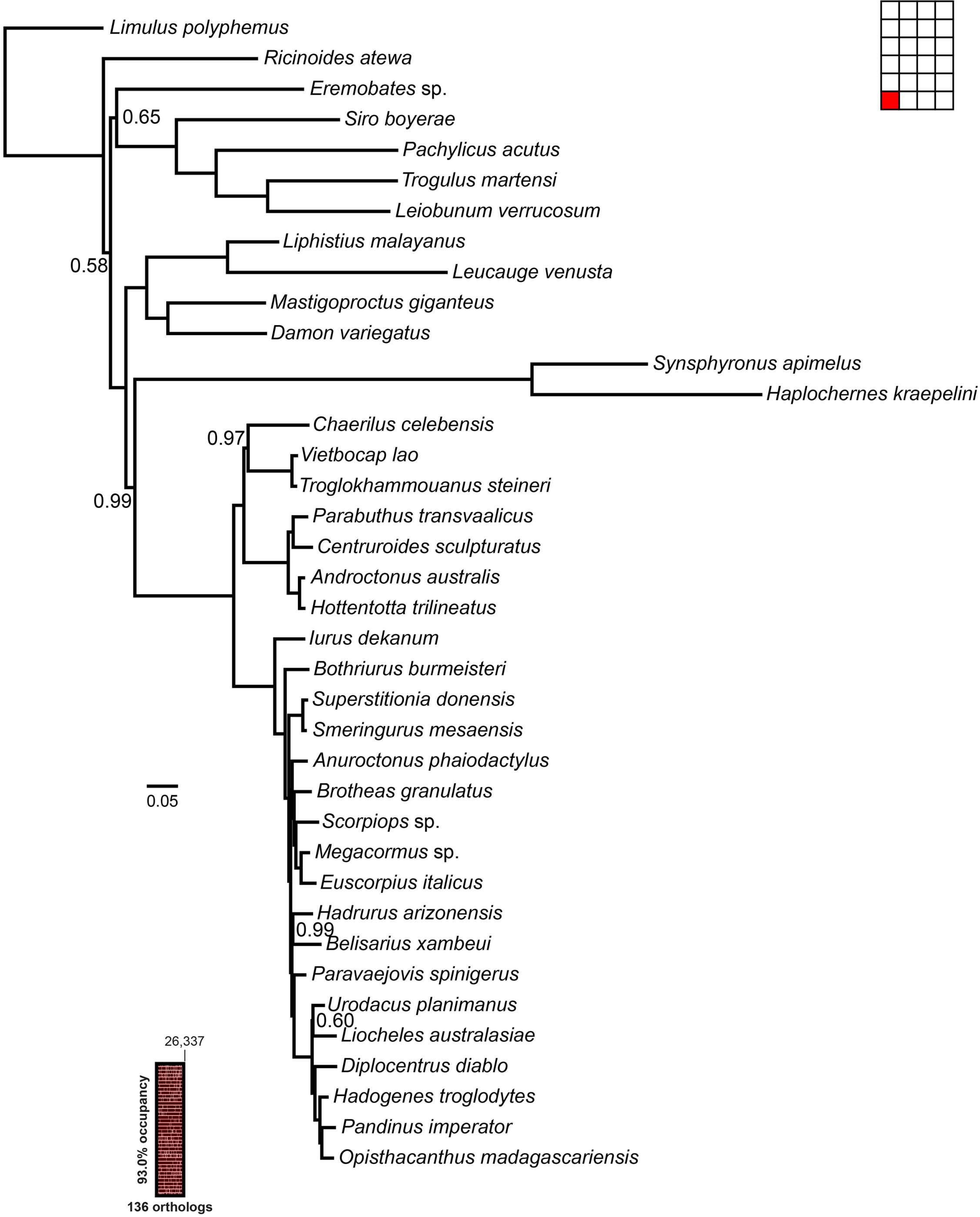

Figure S14. Tree topology based on Bayesian inference analysis of 599 orthologs (Matrix 2). Numbers on nodes indicate posterior probabilities. Unlabelled nodes correspond to posterior probabilities of 1.00.

Figure S15. Tree topology based on maximum likelihood analysis of 67 orthologs (Matrix 11). Numbers on nodes indicate bootstrap resampling frequencies.

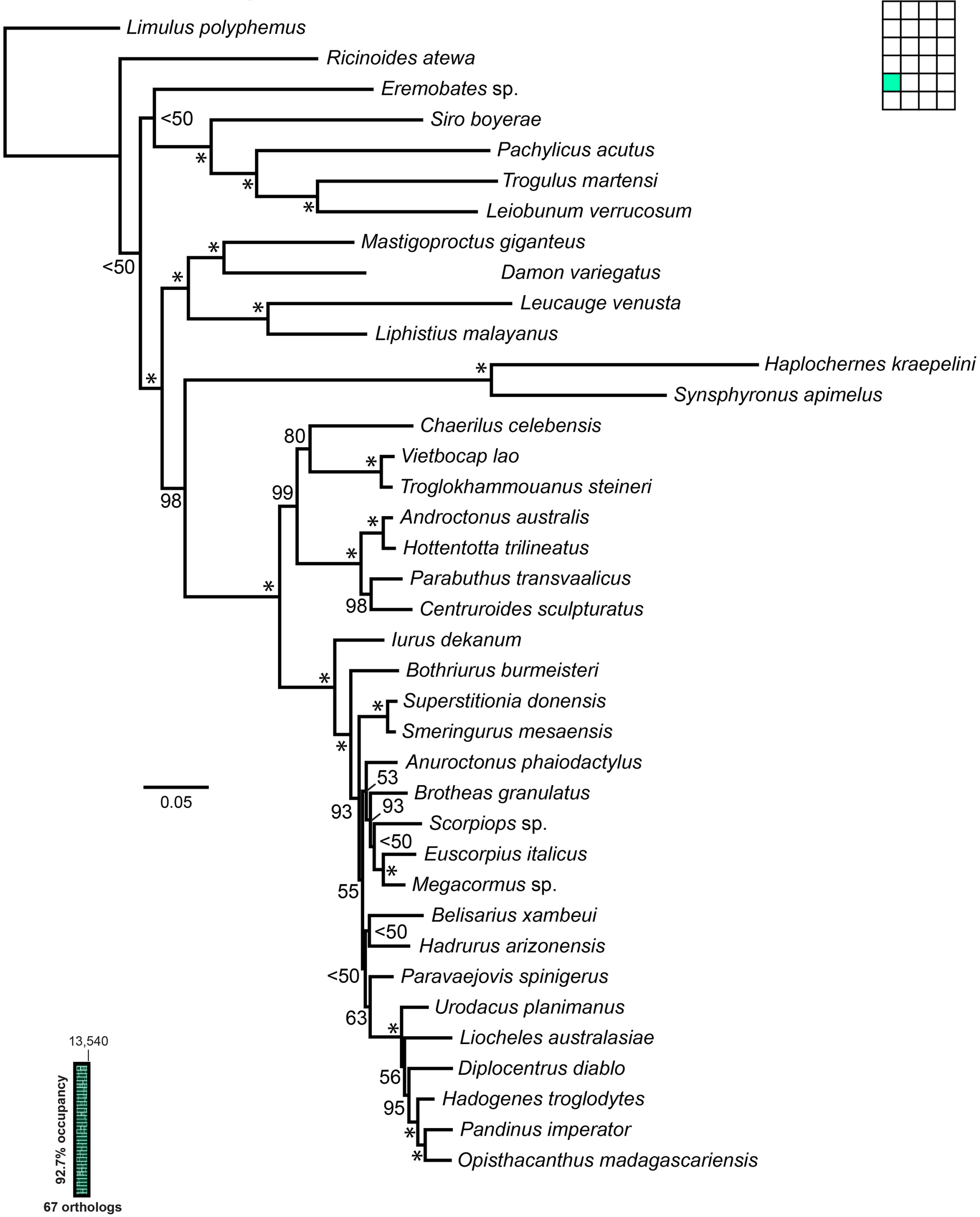

Figure S16. Tree topology based on maximum likelihood analysis of 280 orthologs (Matrix 12). Numbers on nodes indicate bootstrap resampling frequencies.

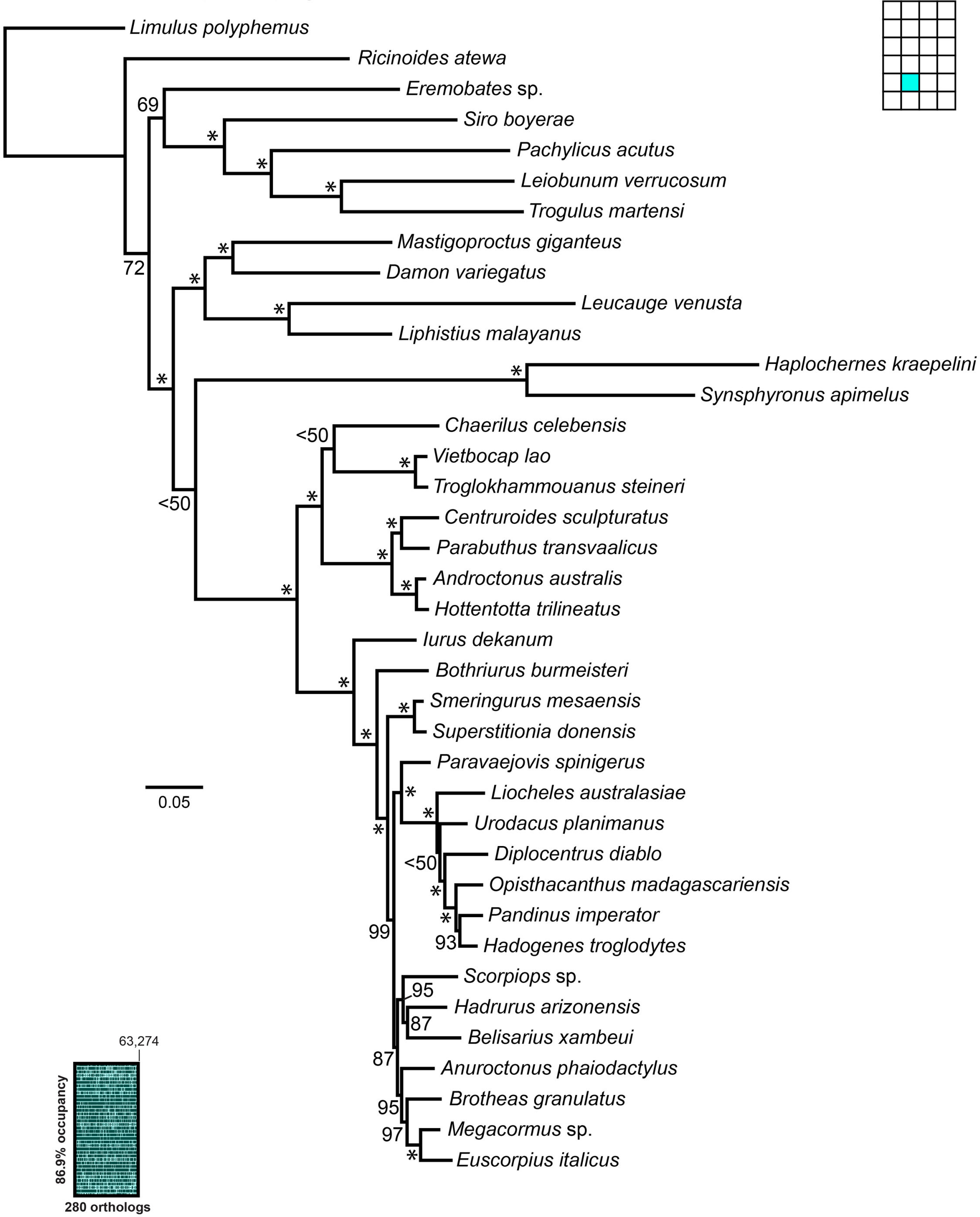

Figure S17. Tree topology based on maximum likelihood analysis of 689 orthologs (Matrix 13). Numbers on nodes indicate bootstrap resampling frequencies.

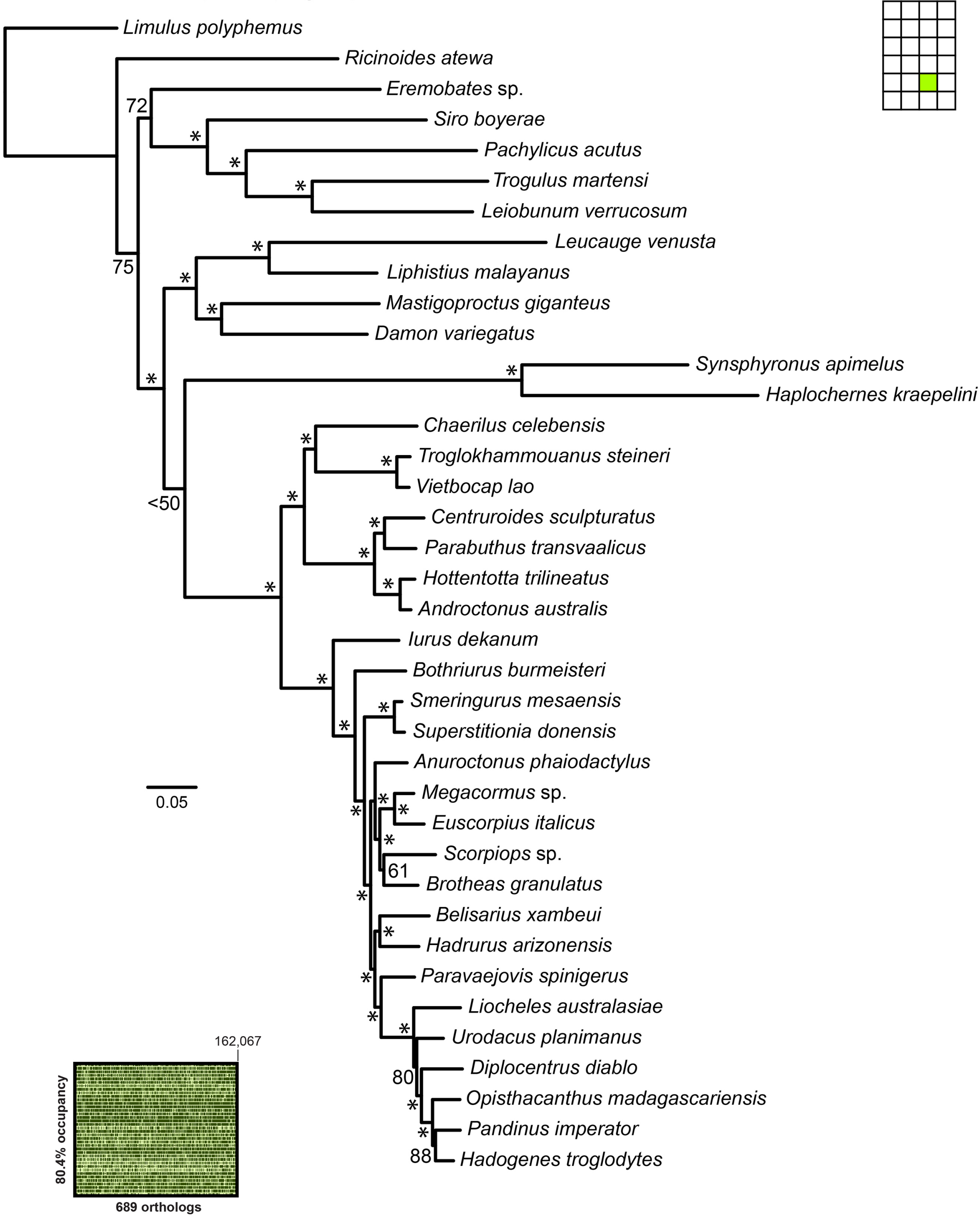

Figure S18. Tree topology based on maximum likelihood analysis of 1,725 orthologs (Matrix 14). Numbers on nodes indicate bootstrap resampling frequencies.

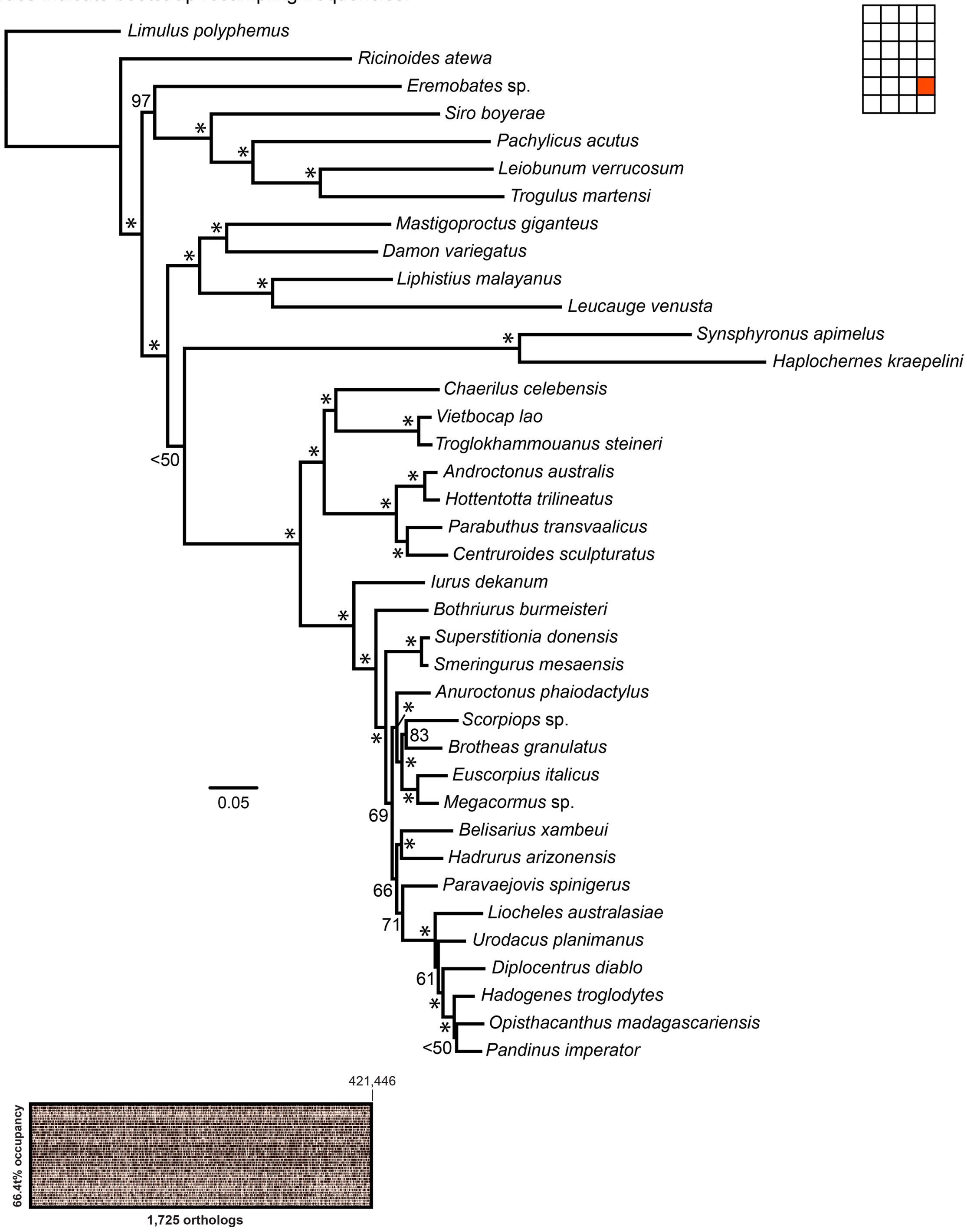

Figure S19. Tree topology based on maximum likelihood analysis of 136 orthologs (Matrix 1) under a mixed branch length model of heterotachy.

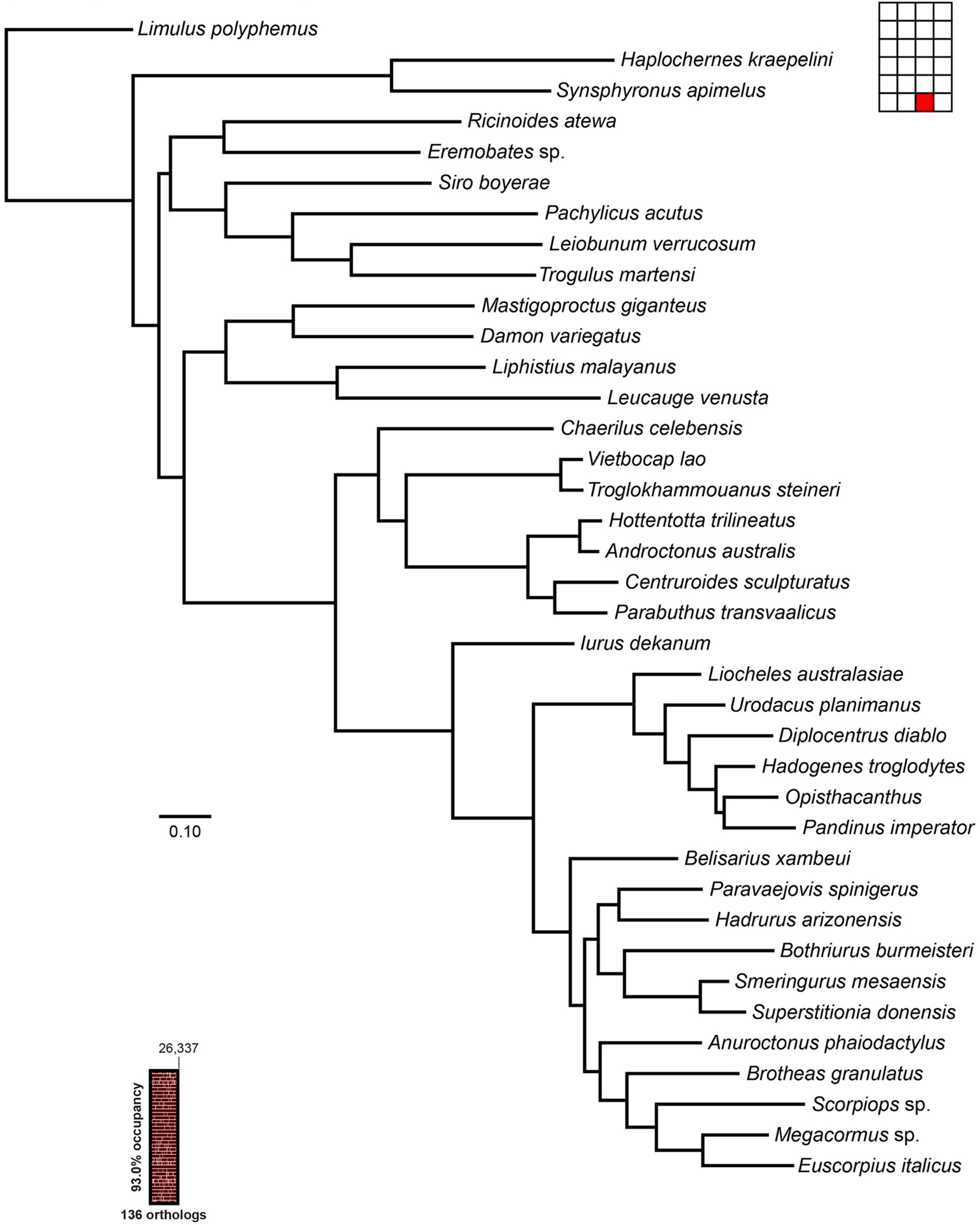

Figure S20. Tree topology based on maximum likelihood analysis of 67 orthologs (Matrix 11) under a mixed branch length model of heterotachy.

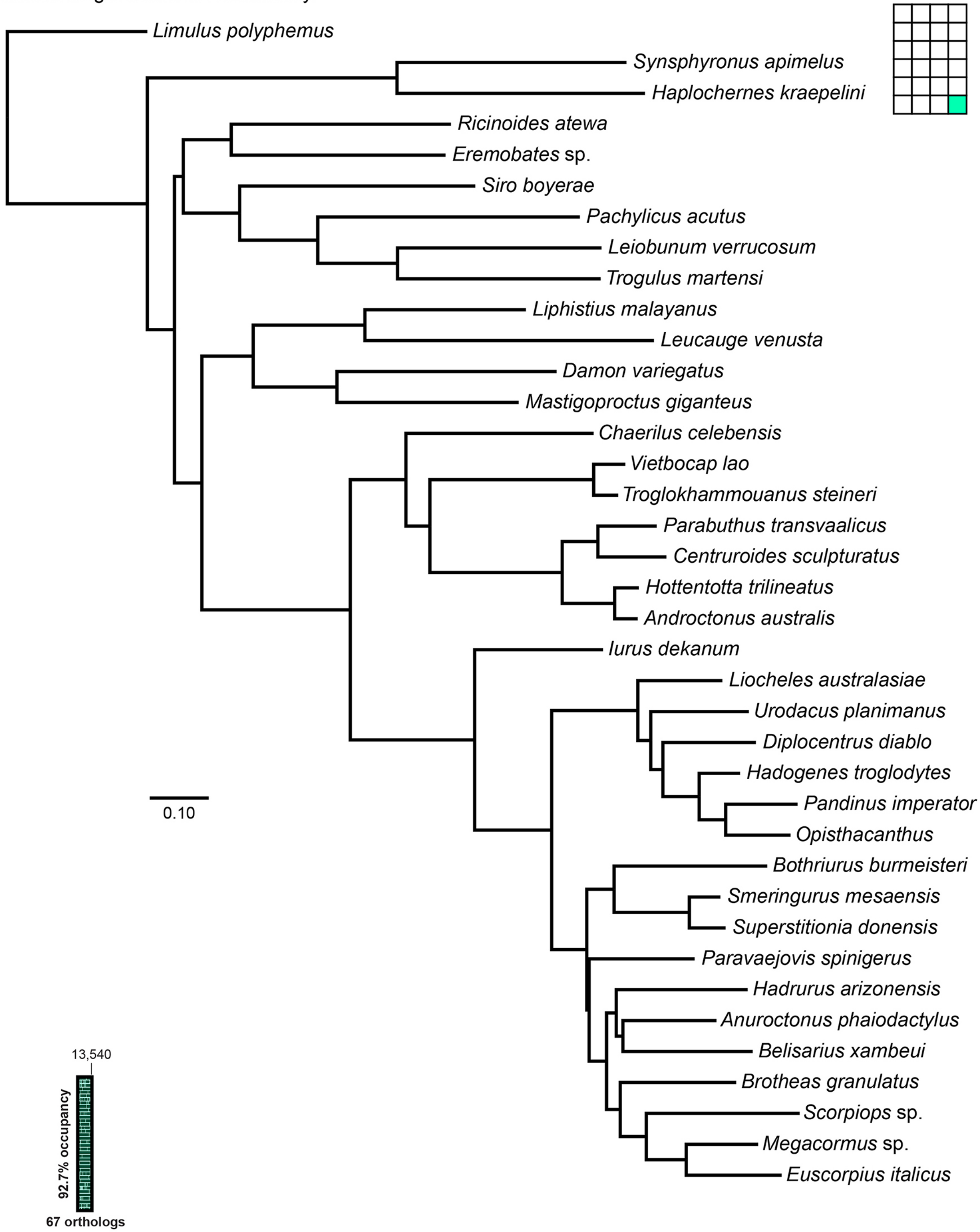

Figure S21. (*a*) Distributions of patristic distances for all terminals from the node that excludes *Limulus polyphemus*, *Ricinoides atewa*, and *Eremobates* sp. Red highlight indicates scorpion terminals. (*b*) Inset: Distributions of same patristic distances, portrayed as histograms. Scorpions are depicted with red, and outgroups with blue.

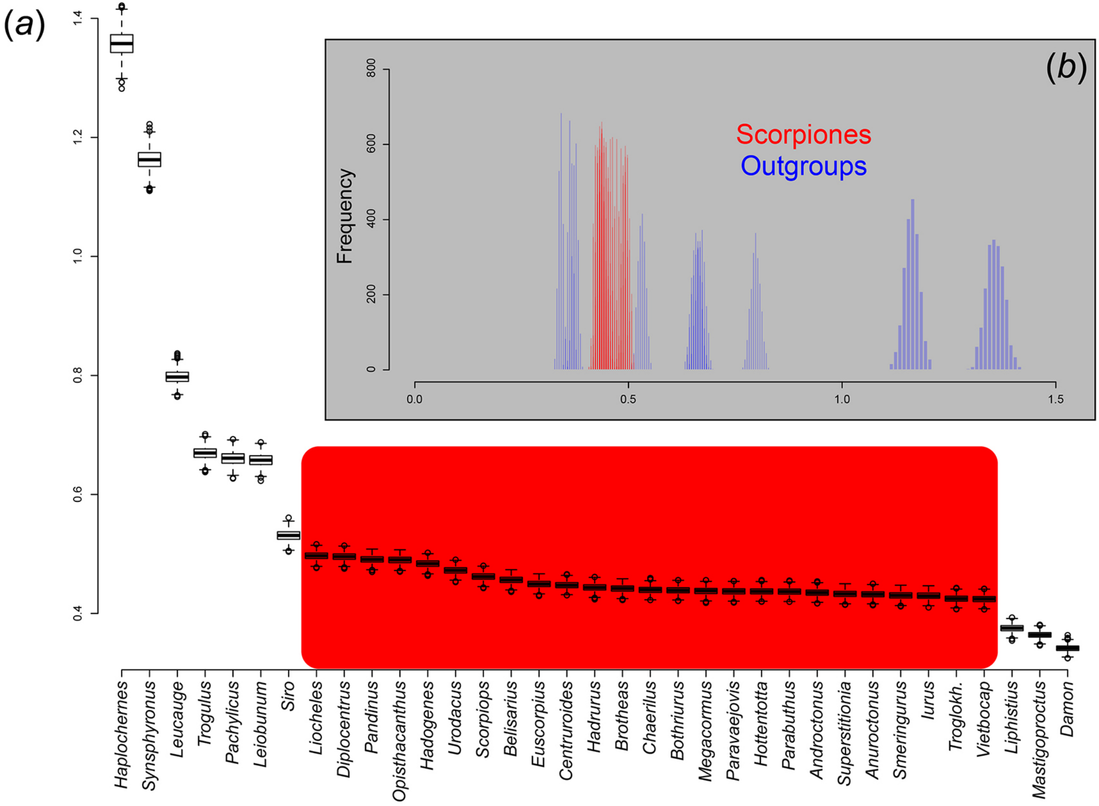

Figure S22. Tree topology based on maximum likelihood analysis of 1,557 orthologs, showing relative support from gene trees in Matrix 3. For each node, the upper number indicates the count of congruent gene trees; the lower number indicates the count of potentially informative genes. Right: Counts mapped for alternative hypotheses.

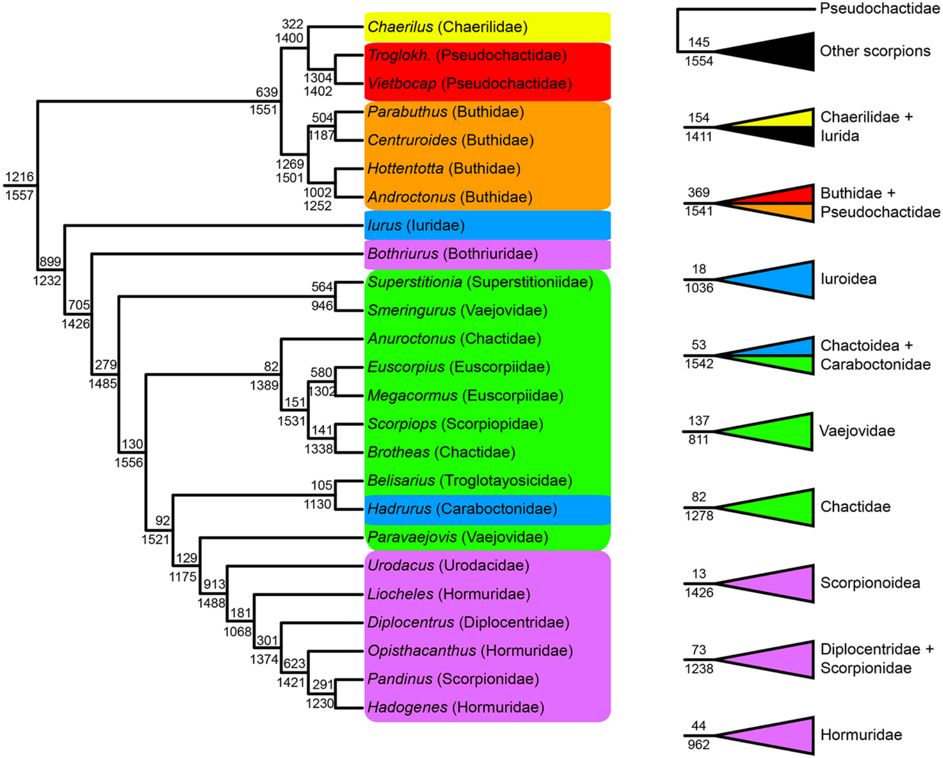

Figure S23. Tree topology based on maximum likelihood analysis of 1,557 orthologs, showing relative support from gene trees in Matrix 4. For each node, the upper number indicates the count of congruent gene trees; the lower number indicates the count of potentially informative genes. Right: Counts mapped for alternative hypotheses.

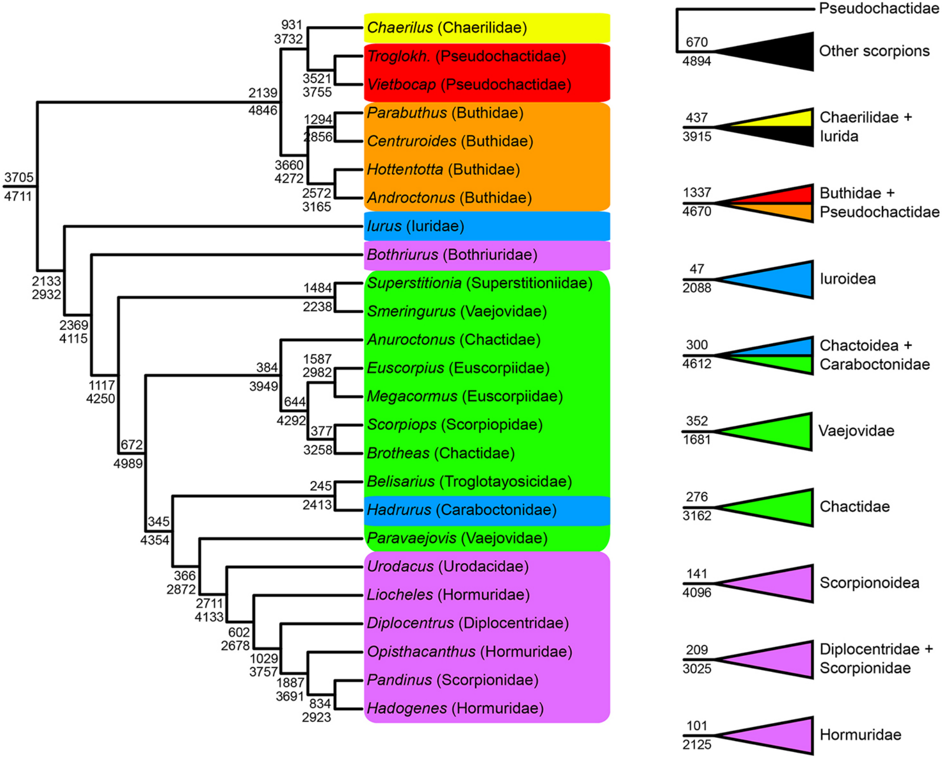

Figure S24. Supernetwork representation of quartets derived from individual ML gene trees, for three different data sets: (a) Matrix 2, (b) Matrix 3, and (c) Matrix 4. Phylogenetic conflict is represented by reticulations. Arrowheads indicate reticulations at the base of Buthida and within Iurida. Edge lengths correspond to quartet frequencies.

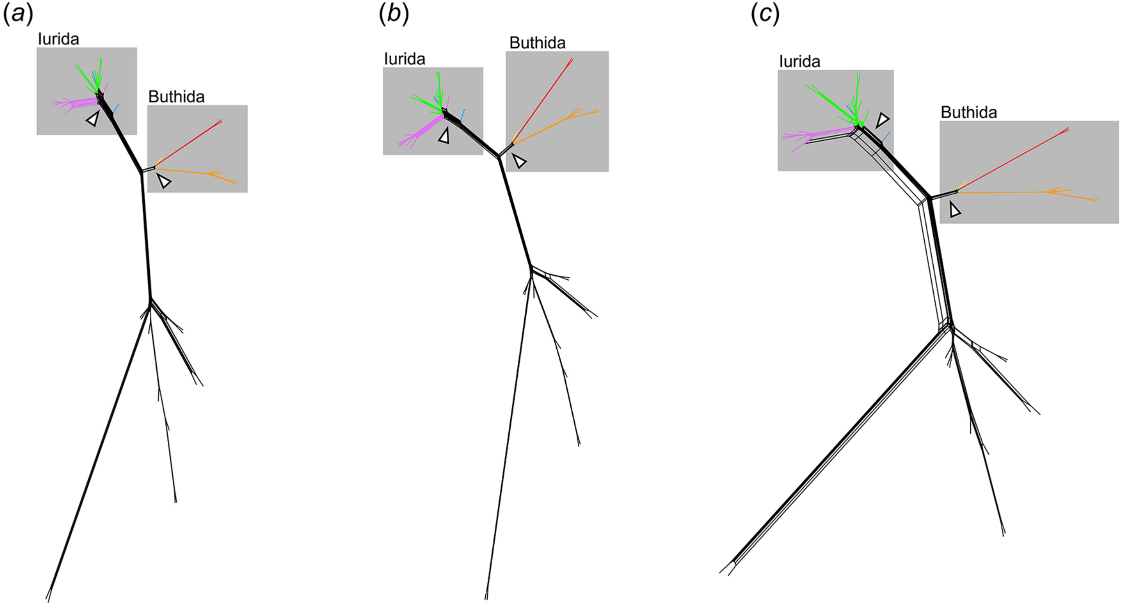

Figure S25. Paucity of morphological characters consistent with the molecular tree topology and informative of interfamilial relationships. Shading of squares indicates character states of morphological characters. Scoring of morphological characters is provided in table S3.

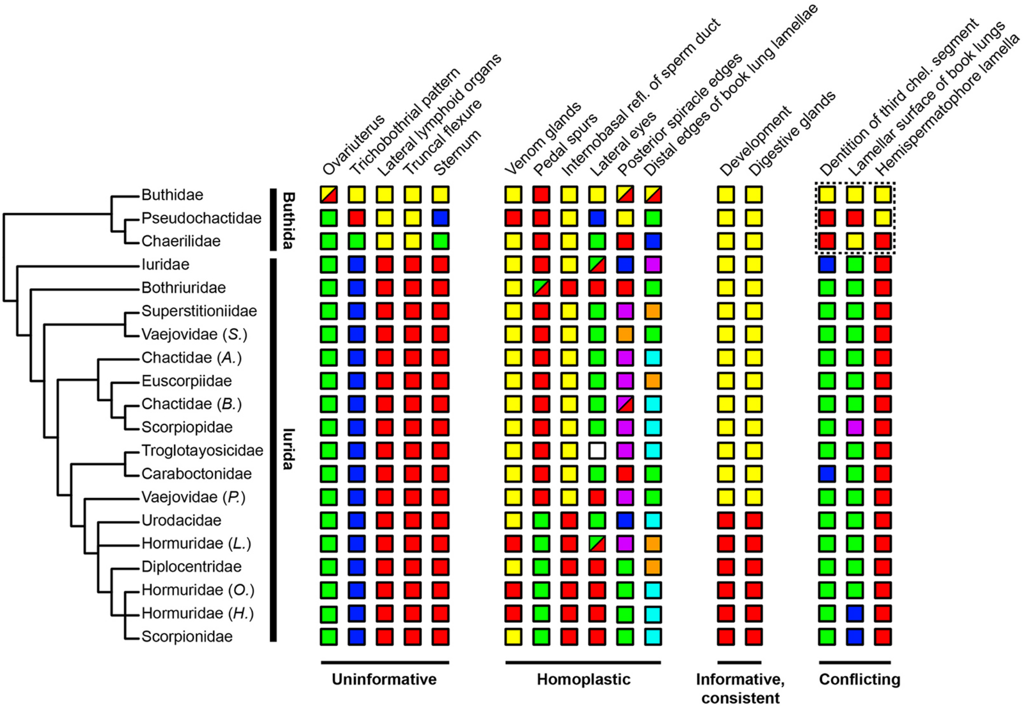

Figure S26. (*a*) Design of permutation-based test for random distribution of missing data. Parsimony scores are calculated for each gene, coding absence as state 0 and presence as state 1. Empirical cases of two orthogroups (#5016 and #5018) with 19 sequences present and different parsimony scores. (*b*) Missing data are determined to be non-randomly (*e.g.*, #5018) or randomly (*e.g.*, #5016) distributed for each gene, relative to a null distribution generated from reshuffling terminals 1,000 times. (*c*) Cumulative number of genes with non-randomly distributed missing data (NDMD) and number of taxa by each orthogroup, ranked in order of taxon occupancy (most to least). Colours indicate key data sets analysed in this study. *p*(NDMD) indicates proportion of each supermatrix that is comprised of genes with non-randomly distributed missing data. (*d*) Cladogram indicating 50% majority rule consensus of bootstrap resampling replicates from 4,008-gene supermatrix with randomly distributed missing data. Numbers on nodes in indicate bootstrap resampling frequencies.